Int. J. Electrochem. Sci., 12 **(2017)** 7537 – 7546, doi: 10.20964/2017.08.75

International Journal of
ELECTROCHEMICAL
SCIENCE
www.electrochemsci.org

Corrosion Inhibition of Carbon Steel in the presence of N,N'-bis(1-phenylethanol)diaminobutane in HCl

Kun Cao[*], *Qian Wang*, *Tian Tian*

Department of Chemistry & Chemical Engineering, Neijiang Normal University, Neijiang, Sichuan, 641112, PR China
[*]E-mail: kevin_cao0811@126.com

Received: 16 May 2017 / *Accepted:* 14 June 2017 / *Published:* 12 July 2017

Carbon steel is an important metal for structure and machines and is easier to be corroded in acidic medium. In this study, N,N'-bis(1-phenylethanol)diaminobutane (BPDAB) was synthesized and used as the corrosion inhibitor for carbon steel in 1 mol/L HCl solution. The inhibition performance of BPDAB was unvestigated by weigh loss test and electrochemical methods. The results of this study showed that the corrosion rate of carbon steel decreased by adding inhibitor to the acid solution, and the inhibition efficiency reached the maximum value of 97.6% with 0.3 mmol/L of BPDAB by electrochemical impedance spectroscopy. The Langmuir adsorption isotherm was used to fit the experimental data, and the results showed that, the spontaneous adsorption of inhibitor molecules on the carbon steel surface, and the adsorption mechanism follows a typical of chemisorption process via the formation of a coordinate bond.

Keywords: Corrosion inhibitor; Electrochemical methods; Carbon steel; Diaminobutane; Quantum chemical calculation

1. INTRODUCTION

Water scale and corrosion products in boiler or heat exchanger could reduce the heat transfer effeciency or even lead to accidents, raising questions on production safety. Therefore, the system should be cleaned with a chemical solution. Most of the scale deposits are formed by insoluble metal salts. HCl solution is one of the most widely used cleaning solution and it could cause a serious corrosion problem, significantly increasing the production costs from the instruction damage, safety measurements, and environmental pollution. To reduce the impact of corrosion, many anticorrosion technologies are used, and corrosion inhibitor is one of the most economical and effective methods[1,2]. Corrosion inhibitors containing N atoms or aromatic ring exhibited excellent corrosion efficiency[3-7].

Diamines compounds and their derivatives have been investigated as corrosion inhibitors for many commercial metals [8-11]. Silva used N,N'-bis(salicylidene)-1,2-ethylenediamine, ethylenediamine and salicylaldehyde as inhibitors for carbon steel in 1.0 mol/L HCl solution, and the results showed that the corrosion inhibition efficiency of the Schiff based compound is higher than those of ethylenediamine and salicylaldehyde[12]. Qu studied the EDTA-2Na and the complex inhibitor with benzotriazole, indicating a low efficieny of EDTA, and the efficiency increased by adding benzotriazole[13]. Another study, showed that the corrosion rate of carbon steel in EDTA solution reached 16.6 mm/a[14].

In this study, N,N'-bis(1-phenylethanol)diaminobutane (BPDAB) including two aromatic rings, as well as oxygen and nitrogen atoms equipped with unshared electron pairs was synthesized and its inhibition efficiency against steel corrosion in 1 mol/L HCl acid solution was investigated. The corrosion inhibition efficiency, was assessed by electrochemical techniques and theoretical studies.

2. EXPERIMENTAL

2.1 Synthesis of inhibitor

BPDAB was synthesized in our laboratory by the Azizi method[15]. The concentration of the BPDAB was in the range from 0.03 mmol/L to 0.3 mmol/L in 1 mol/L HCl solution.

2.2 Weight loss test

Carbon steel was cut into a sheet of 50 × 25 × 2 mm^3, and all the specimens were abraded using a sandpaper from 600 to 1000 grit, measured the dimensions and weighed, after that, the every three speciments were immersed in 1 mol/L HCl solution without or with BPDAB for 3 h, and then, each smaple was taken out from the solution, removed the corrosion production in distilled water and acetone, finally dried and weighed after 24 h. The corrosion rate (v, mg m^{-2} h^{-1}) and the inhibition efficiency (IE_W) were calculated by Eqs. 1 and 2, respectively.

$$v = \frac{W_0 - W}{s \cdot t} \qquad \text{(Eq. 1)}$$

$$IE_w = \frac{v_0 - v}{v_0} \times 100\% \qquad \text{(Eq. 2)}$$

where W_0 and W are the weight of carbon steel immersed in the solution without or with inhibitor, respectively.s is the area of the sample surface, t is the immersing time, v_0 and v are the corrosion rate of the carbon steel in the solution in the absence or presence of the inhibitor, respectively.

2.3. Electrochemical experiments

Electrochemical impedance spectra and polarization curves were recorded using a three-electrode cell system. The platinum plate electrode and saturated calomel electrode (SCE) connect

with a Luggin capillary were used as the counter and reference electrodes, respectively. The working electrode was carbon steel which was cut into cube and embedded in epoxy resin with an exposed surface area of 1 cm^2. Before all the electrochemical test, the working electrodes should be abraded, then degreased ultrasonically in acetone, and dried naturely.

The electrochemical tests were performed and the curves were analyzed using an Ivium electrochemical workstation and software. The polarization curves were scanned from –250 to +250 mV (versus open circuit potential) at a scanning rate of 0.5 mV/s. EIS measurements were conducted in the frequency range from 100 kHz to 10 mHz. The inhibition efficiency based on the corrosion current density or EIS parameters was calculated by Eqs. 3 and 4

$$IE_{\mathrm{i}} = \frac{i_{0,\mathrm{corr}} - i_{\mathrm{corr}}}{i_{0,\mathrm{corr}}} \times 100\% \qquad \text{(Eq. 3)}$$

$$IE_{\mathrm{R}} = \frac{R_{\mathrm{ct}} - R_{0,\mathrm{ct}}}{R_{\mathrm{ct}}} \times 100\% \qquad \text{(Eq. 4)}$$

where i_{corr} and $i_{0,\mathrm{corr}}$ are the corrosion current density of carbon steel with and without the inhibitor in 1 mol/L HCl solution, respectively, and R_{ct} and $R_{0,\mathrm{ct}}$ are the charge transfer resistance with/without inhibitor, respectively.

2.4. Quantum chemical calculation

The molecular structure of the inhibitor and energy of the orbit were fully optimized by DFT method using Gaussian software. The quantum chemical parameters, such as the orbital energy distribution, energy gap and fraction of transferred electrons (ΔN) were considered.

3. RESULTS AND DISCUSSION

3.1 Weight loss test

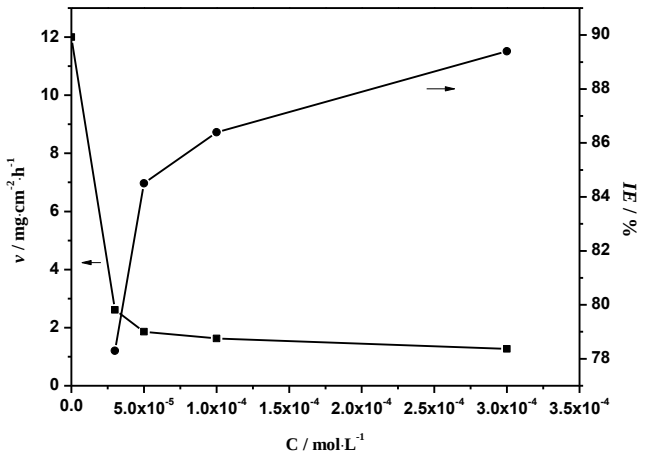

Figure 1. Weight loss results of carbon steel with different concentrations of inhibitor

Fig.1 shows the corrosion rate and corrosion inhibition efficiency of the carbon steel in HCl solution. From the curves, it is benificial to reduce the corrosion rate by adding the corrosion inhibitor, and the inhibition efficiency was higher than 89% at the concentration of 0.3 mmol/L.

3.2 EIS measurement

Carbon steel was immersed in 1 mol/L HCl solution with or without inhibitor for 30 min, then followed by recording the data, and the Nyquist plots are shown in Fig. 2. All the impedance plots in Fig. 2 clearly show a single irregular depressed semi-circle, indicating a non-ideal capacitive behavior at the interface between the electrode surface and liquid [16]. The non-ideal behavior can be attributed to the charge transfer reaction and the formation of inhibitor film [17,18]. The impedance was fitted to an equivalent electrical circuit shown in Fig. 3, comprising a parallel connection between the charge transfer resistance (R_{ct}) and the double layer capacitance (C_{dl}) and these impedance elements were connected to the electrolyte resistance (R_s) in series. The inhibition efficiency and other fitted impedance parameters are listed in Table 1. The data in Table 1 show that the R_{ct} increased, whereas C_{dl} decreased with adding inhibitors in 1mol/L HCl solutions, and the trends became more obvious with increasing inhibitor concentration. The increase in R_{ct} was due to decrease in the active surface which associated with corrosion reaction. The decreased C_{dl} values can result from the adsorption of inhibitor on the carbon steel surface to form a protective layer[19], increasing the thickness of the electrical double layer or decreasing of the local dielectric constant by substituting water molecules (with higher dielectric constant) with inhibitor molecules (with lower dielectric constant).

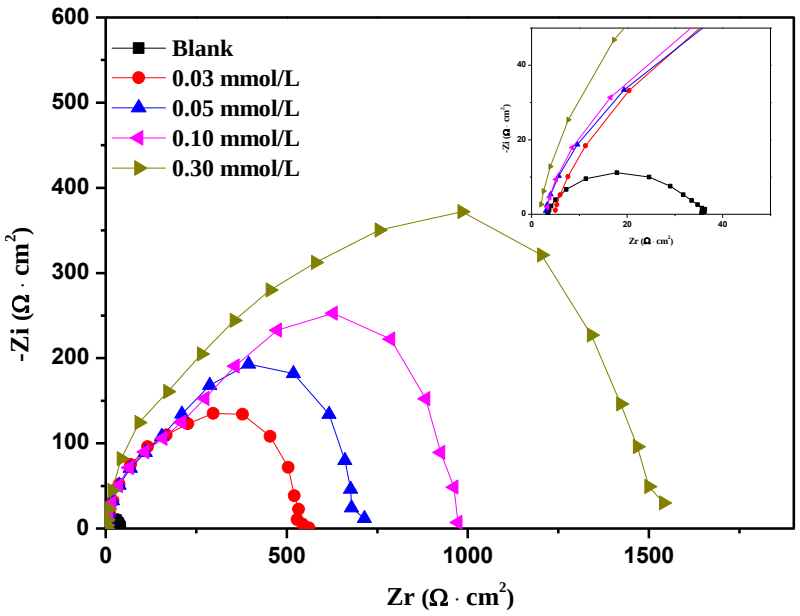

Figure 2. Nyquist plots of carbon steel in 1 mol/L HCl solution with different concentrations of inhibitor

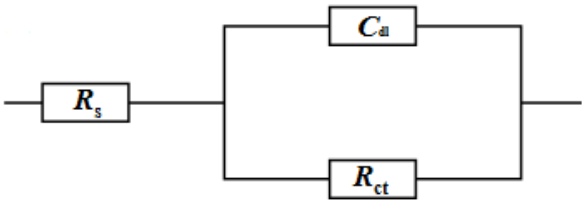

Figure 3. Equivalent circuit of Nyquist plots

Table 1. Impedance parameters of carbon steel in 1 mol/L HCl solution with different concentrations of inhibitor

C (mmol/L)	R_s (Ω cm^2)	C_{dl} (μF/cm$^{2)}$	n	R_{ct} (Ω cm^2)	IE_R (%)
Blank	2.173	125.2	0.78	32.0	
0.03	3.664	62.5	0.70	516.7	93.8
0.05	1.727	61.29	0.68	660.5	95.2
0.10	2.899	48.54	0.61	933.8	96.6
0.30	1.666	27.18	0.70	1355	97.6

3.3 Potentiodynamic polarization curves

Potentiodynamic polarization measurements allow determining the corrosion inhibition mechanism of the anodic dissolution of carbon steel and cathodic hydrogen ion reduction. The polarization curves in the potentials range ±250 mV relating to the corrosion potential E_{corr} with or without inhibitors are shown in Fig. 4. The results of the polarization curves extrapolation for mild steel in 1 mol/L HCl containing various concentrations of the inhibitors are summarized in Table 2. The polarization curves show that the E_{corr} values did not shift definitely with increasing concentration, but both the cathodic and the anodic current decreased significantly. This phenomenon indicates that both anodic metal dissolution and cathodic hydrogen evolution reactions are suppressed via the coverage of inhibitor molecules on the metal surface. The displacement in E_{corr} (ΔE_{corr}) with and without inhibitor was less than 85 mV. Therefore, the inhibitor was as a mix-type inhibitor[20-22], indicating that the inhibitor works significantly and effectively by the hydrogen evolution reaction on the cathode, slowing the dissolution rate of carbon steel. Such behavior supports and proves that the inhibitor could adsorb onto the steel surface, forming a film for hindering mass and charge transfer at the anodic and cathodic interface [23].

The cathodic (β_c) and anodic Tafel slopes (β_a) were obtained by extrapolation, and the values barely changed with increasing inhibitor concentration, indicating that the presence of inhibitor do not change the mechanism of hydrogen evolution and metal dissolution [24].

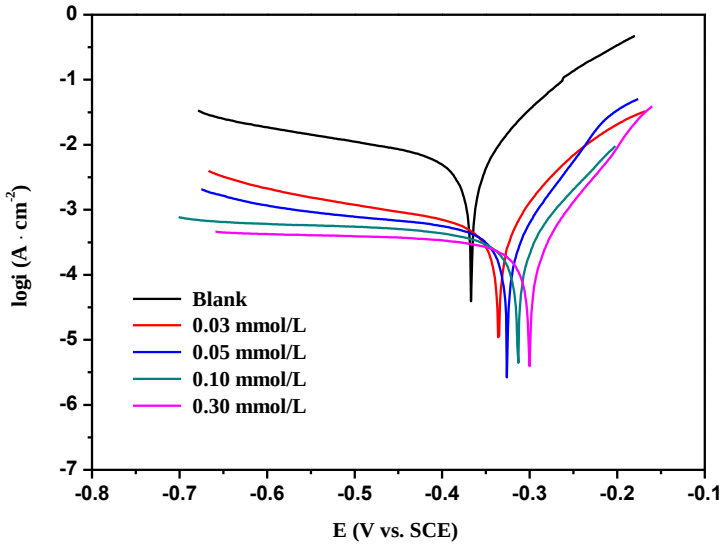

Figure 4. Tafel curves of carbon steel in 1 mol/L HCl solution with different concentrations of inhibitor

Table 2. Tafel parameters of carbon steel in 1 mol/L HCl solution with different concentrations of inhibitor

C (mmol/L)	E_{corr} (V vs. SCE)	i_{corr} （mA/cm^2）	β_c （mV/dec）	β_a （mV/dec）	IE_i （%）
Blank	-0.371	1.252	78	32	
0.03	-0.342	0.1254	70	31	90.0
0.05	-0.330	0.1139	68	35	90.9
0.10	-0.312	0.09855	61	33	92.1
0.30	-0.298	0.08569	70	35	93.2

3.4 Adsorption isotherm

Corrosion inhibitor protects the carbon steelvia the adsorption process of inhibitor on the steel surface. In fact, the adsorption process is a process of inhibitor molecules replacing water molecules on the steel surface[25].

The adsorption process can be fitted by adsorption isotherm. Four types of adsorption model were used to fit the adsorption of inhibitor on the steel surface, and the best correlation was obtained by the Langmuir adsorption isotherm. The relationship between θ *and* C obeyed the following equation:

$$\frac{C}{\theta} = \frac{1}{K_{ads}} + C \quad \text{(Eq. 5)}$$

$$\Delta G_{ads} = -RT \ln\left(55.5 K_{ads}\right) \quad \text{(Eq. 6)}$$

where K_{ads} is the equilibrium constant of the inhibitor adsorption process, and ΔG^0_{ads} is the standard free energy of adsorption.

The fitting curves according to the weight loss test and electrochemical measurement are shown in Fig. 5. The data calculated from the intercept are listed in Table 3.

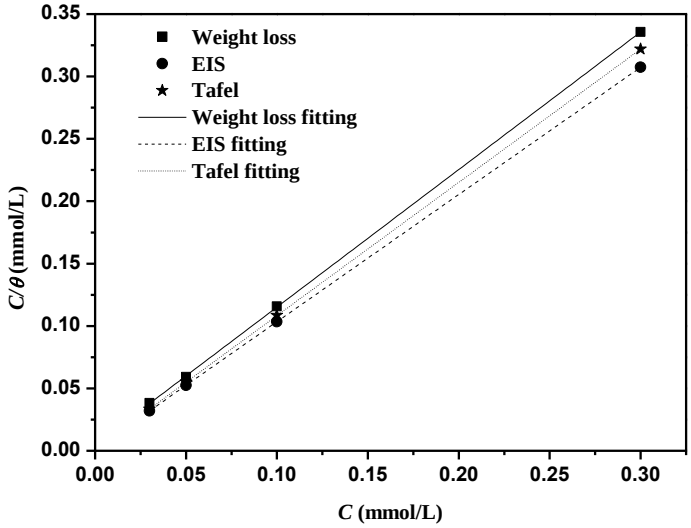

Figure 5. Langmuir adsorption isotherms of carbon steel in HCl solution

Table 3. Thermodynamic parameters of carbon steel in HCl solution

	R^2	K_{ads} (10^4 L/mol)	ΔG_{ads} (kJ/mol)
Weight loss	0.9989	20.4498	-40.25
EIS	0.9996	67.1141	-43.19
Tafel	0.9995	65.3594	-43.13

The negative value of ΔG^0_{ads} indicates the spontaneous adsorption of inhibitor on the steel surface. In general, the value of ΔG^0_{ads} more negative than -40 kJ/mol, indicating a chemisorption process, which involves the sharing or transferring of electrons from the inhibitor to metal surface [26, 27]. In the view of our previous research [28, 29, 30], the electrons provided by the N atoms and aromatic ring, form the coordination bond with the vacant hybrid orbital of Fe atoms.

3.5 Quantum chemical calculation

The active adsorption center of the inhibitor molecule on the metal surface relate to the ability to gain or loss electrons. According to the frontier molecular orbital theory, the energy of highest occupied molecular orbit (E_{HOMO}) is associated with the tendency of electron donation at lower energy, and the energy of lowest unoccupied molecular orbit (E_{LUMO}) is associated with electrons acceptance

[31]. Therefore, a lower value of ΔE ($\Delta E=E_{LUMO}-E_{HOMO}$) will cause a higher value of inhibition efficiency [32]. The HOMO and LUMO were fully optimized by the DFT method using 6-31G* basis set, as shown in Fig. 6.

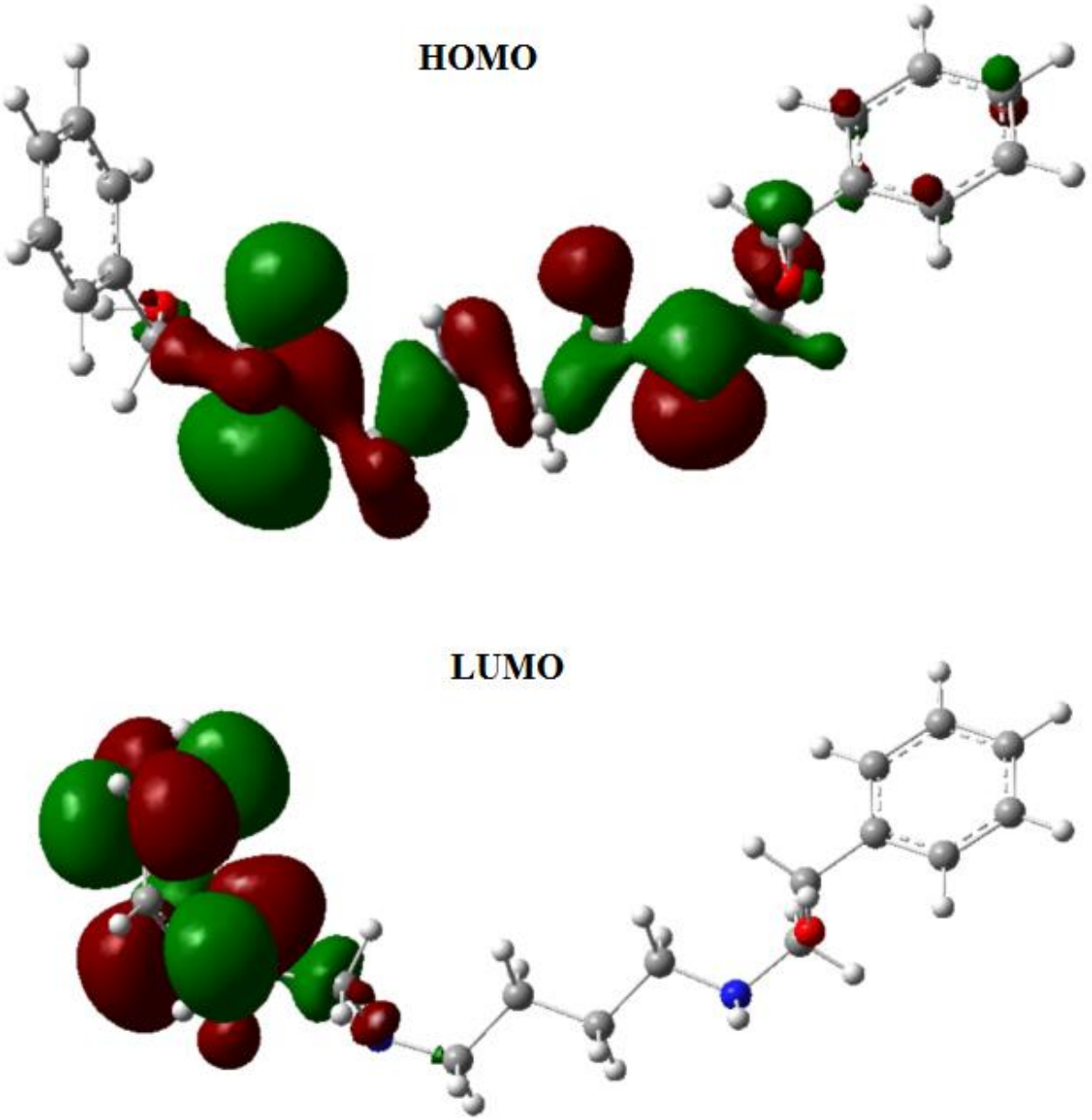

Figure 6. Quantum chemical calculation results of BPDAB

The calculated HOMO and LUMO energy levels are listed in Table 4. Other quantum chemical parameters, such as ionization potential (I), and the electron affinity (A) calculated from the E_{HOMO} and E_{LUMO} are also listed in Table 4. Fraction of transferred electrons (ΔN) was calculated by χ and η, representing the absolute electro negativity and the absolute hardness, respectively, by the following

equation:

$$\Delta N = \frac{\chi_{Fe} - \chi_{inh}}{2(\eta_{Fe} + \eta_{inh})} \quad \text{(Eq. 7)}$$

where χ_{Fe} or χ_{inh} are the electro negativity of carbon steel or BPDAB, respectively; η_{Fe} or η_{inh} are the global hardness of carbon steel or BPDAB. The value of χ_{Fe} and η_{Fe} are 7 eV and 0 eV, as reported in literature [33].

Table 4. The quantum chemical parameters of BPDAB

	E_{HOMO} (eV)	E_{LUMO} (eV)	ΔE	I=-E_{HOMO}	A=-E_{LUMO}	χ	η	ΔN
BPDAB	-5.529	-1.582	3.947	5.529	1.582	3.556	1.974	0.8723

Compared to the former studies [34], the BPDAB had higher E_{HOMO} and lower E_{LUMO}, indicating that it was easier to donate electrons to appropriated acceptor molecule. It is found that the electron of the inhibitor transferred to the Fe atom when $\Delta N > 0$. On the contrary, such transfer can be operated from the metal surface to the inhibitor when $\Delta N < 0$ [35]. In contrast, when $\Delta N < 3.6$, the inhibition efficiency increases with increasing electron-donating ability of the molecule to the surface of the carbon steel. The value of ΔN was found to be 0.8723, illustrating that the inhibitor can share electrons with carbon steel by forming the coordinate bond.

4. CONCLUSIONS

(1) BPDAB is an effective inhibitor for carbon steel in 1 mol/L HCl solution. The inhibition efficiency increases with increasing inhibitor concentration and reaches the maximum values of 97.6% (EIS test) and 93.2% (Tafel curves) at the optimum BPDAB concentration of 0.3 mmol/L.

(2) The polarization curves suggest that BPDAB acts as mixed-type inhibitors. The electrochemical impedance study showed that corrosion inhibition of carbon steel in 1 mol/L HCl solution takes place by the adsorption process.

(3) The large negative values of ΔG^0_{ads} indicated that the adsorption of the BPDAB on the carbon steel surface is spontaneous, and the adsorption mechanism follows a typical chemisorption process. The adsorption of the BPDAB obeyed the Langmuir adsorption isotherm.

(4) The calculated quantum chemical parameters such as ΔE and ΔN support the good inhibition performance of the BPDAB.

ACKNOWLEDGEMENTS

The author gratefully acknowledges the support of Key Founding of Sichuan Province Education Department (17ZA0220), the Doctor Founding of Neijiang Normal University (No. 15B13) and the Opening Foundation of the Key Laboratory of Fruit Waste Treatment and Resource Recycling of the Sichuan Province College (KF17004).

References

1. H. R. Obayes, A. A. Al-Amiery, G. H. Alwan, T. A. Abdullah, A. A. H. Kadhum and A. B. Mohamad, *J. Mol. Struct*., 1138 (2017) 27.
2. Y. J. Qiang, S. T. Zhang, L. Guo, X. W. Zheng, B. Xiang and S. J. Chen, *Corros. Sci*., 119 (2017) 68.
3. M. ElBelghiti, Y. Karzazi, A. Dafali, B. Hammouti, F. Bentiss, I. B. Obot, I. Bahadur and E. E. Ebenso, *J. Mol. Liq*., 218 (2016) 281.
4. M. E. Belghiti, Y. Karzazi, A. Dafali, I. B. Obot, E. E. Ebenso, K. M. Emran, I. Bahadur, B. Hammouti and F. Bentiss, *J. Mol. Liq*., 216 (2016) 874.
5. L. Guo, S. H. Zhu, S. T. Zhang, Q. He and W. H. Li, *Corros. Sci*., 87 (2014) 366.
6. P. Han, C. F. Chen, H. B. Yu, Y. Z. Xu and Y. J. Zheng, *Corros. Sci*., 112 (2016) 128.
7. C. Zhang, H. B. Duan and J. M. Zhao, *Corros. Sci*., 112 (2016) 160.
8. M. Al-Sabagh, N. M. Nasser, E. A. Khamis and T. Mahmoud, *Egypt. J. Petrol*., 26 (2017) 41.
9. A. Manivel, S.r Ramkumar, J. J. Wu, A. M. Asiri and S. Anandan, *J. Environ. Chem. Eng*., 2 (2014) 463.
10. N. Zakiah, N. Hashim, K. Kassim and Y. Mohd, *APCBEE Procedia*, 3 (2012) 239.
11. R. Laamari, J. Benzakour, F. Berrekhis, A. Abouelfida, A. Derja and D. Villemin, *Arab. J. Chem*., 4 (2011) 271.
12. A. B. Silva, E. D'Elia, J. A. Cunha and P. Gomes. *Corros. Sci*., 52 (2010) 788.
13. Q. Qu, S. Jiang, W. Bai and L. Li, *Electrochim. Acta*, 52 (2007) 6811.
14. J. A. Calderon, G. F. Bonilla and J. A. Carreno, *J. oil, gas altern. energ. source*., 5 (2014) 35.
15. N. Azizi and M. R. Saidi, *Org. Lett*., 7 (2005) 3649.
16. M. Hosseini, S. F. L. Mertens, M. Ghorbani and M. R. Arshadi. *Mater. Chem. Phys*., 78 (2003) 800.
17. C. M. A. Brett, *Corros. Sci*., 33 (1992) 203.
18. E. M. Sherif and S. M. Park, *Electrochim. Acta*, 51 (2006) 1313.
19. B. Qian, J. Wang, M. Zheng and B. Hou, *Corros. Sci*., 75 (2013) 184.
20. G. Quartarone, L. Bonaldo and C. Tortato, *Appl. Surf. Sci*., 252 (2006) 825.
21. L. R. Chauhan and G. Gunasekaran, *Corros. Sci*., 49 (2007) 1143.
22. M. A. Hegazy, *Corros. Sci*., 51 (2009) 2610.
23. A. M. Al-Sabagh, H. M. Abd-El-Bary, R. A. El-Ghazawy, M. R. Mishrif and B. M. Hussein, *Egypt. J. Petrol*., 20 (2011) 33.
24. S. S. Abdel-Rehim, M. A. M. Ibrahim and K. F. Khaled, Mater. Chem. Phys., 70 (2001) 268.
25. M. Sahin, S. Bilgic and H. Yilmaz, *Appl. Surf. Sci*., 195 (2002) 1.
26. F. M. Donahue and K. Nobe, *J. Electrochem. Soc*., 112 (1965) 886.
27. A. Yurt, S. Ulutas and H. Dal, *Appl. Surf. Sci*., 253 (2006) 919.
28. Z. Tao, W. He, S. Wang and G. Zhou, *Indust. Eng. Chem. Res*., 52 (2013) 17891.
29. Z. Tao, W. He, S. Wang, S. Zhang and G. Zhou, *Corros. Sci*., 60 (2012) 205.
30. Z. Tao, W. He, S. Wang, S. Zhang and G. Zhou, *J. Mater. Eng. performance*, 22 (2013) 774.
31. K. Fukui, Theory of Orientation and Stereoselection, Springer-Verlag, (1975) New York, US.
32. G. Gece, *Corros. Sci*., 50 (2008) 2981.
33. R. Kumar, O. S. Yadav, *J. Mol. Liq*., 237 (2017) 413.
34. H. Tian, W. Li, K. Cao and B. Hou, *Corros. Sci*., 73 (2013) 281.
35. R. G. Pearson, *Inorg. Chem*., 27 (1988) 734.

© 2017 The Authors. Published by ESG (www.electrochemsci.org). This article is an open access article distributed under the terms and conditions of the Creative Commons Attribution license (http://creativecommons.org/licenses/by/4.0/).